



# Undigested glycosylated lentil proteins modulate the gut microbiota profile but not the metabolites *in vitro*

Ruth T. Boachie<sup>a,b</sup>, Edoardo Capuano<sup>a,\*</sup>, Teresa Oliviero<sup>a</sup>, Chibuikwe C. Udenigwe<sup>b,c</sup>, Vincenzo Fogliano<sup>a</sup>

<sup>a</sup> Food Quality and Design Group, Wageningen University and Research, 6700 EV Wageningen, The Netherlands

<sup>b</sup> School of Nutrition Sciences, Faculty of Health Sciences, University of Ottawa, Ottawa, Ontario K1H 8M5, Canada

<sup>c</sup> Department of Chemistry and Biomolecular Sciences, Faculty of Science, University of Ottawa, Ottawa, Ontario K1N 6N5, Canada

## ARTICLE INFO

### Keywords:

Maillard reaction  
Plant protein digestibility  
Batch fermentation  
SHIME  
Food protein fermentation  
Dietary advanced glycation end-products (dAGEs)

## ABSTRACT

Glycation enhances plant protein techno-functionality; however, digestibility and the equilibrium between peptides absorbed and those reaching the colon can be altered. This study evaluated how undigested glycosylated lentil proteins, potentially reaching the colon affect the gut microbiota using batch fermentation and the Simulator of Human Intestinal Microbiome Ecosystem (SHIME®). Lentil protein-fructose mixtures were incubated at 60 °C for 0, 24, or 48 h (conjugates labelled LP+Fr0, LP+Fr1, LP+Fr2). Maillard reaction markers increased by over 10-fold and *in vitro* protein digestibility decreased by 23.5 % after 48-h incubation. Short- and branched-chain fatty acids produced by 48 h-fermentation of the insoluble hydrolysates of conjugates were comparable. LP+Fr2 hydrolysates caused 42 % relative increase in Bacteroidetes in the proximal colon of Donor 1 whereas 26 % increase was observed with LP+Fr0 hydrolysates. Bacteria population profile in the colon sections was differentially modulated depending on the donor. Our findings show that the extent of glycation does not affect short- and branched-chain fatty acid levels produced in the colon, while the effect on microbiota population is dependent on host and colon section.

## 1. Introduction

To meet the protein needs of the increasing global population, the variety of food protein sources must be widened. Hence, plant protein sources, such as pulses, continue to receive attention as sustainable alternatives to traditional animal protein sources. Pulses are widely consumed, even in areas where food security is a challenge. Moreover, previous reports have shown that pulse protein hydrolysates can provide beneficial functions, such as blood glucose modulation by inhibiting the activities of  $\alpha$ -amylase,  $\alpha$ -glucosidase, and dipeptidyl peptidase IV (Di Stefano et al., 2019; Olagunju et al., 2021). The health benefits of pulse protein consumption have also prompted an increase in their acceptance in food products.

Beyond their nutritional value, the techno-functional properties of food proteins are relevant in food product applications. Traditional food applications of proteins have been from animal sources; however, due to the need for more sustainable alternatives, pulse proteins are being considered for their suitability in food product applications. The major

challenge of pulse proteins is the compact globular structure of their predominant proteins and their high molecular weight which limit their techno-functionality (Day & Cakebread, 2022; Kutzli et al., 2021). For instance, pulse proteins are mostly seed storage proteins with hydrophobic compact structures, whereas milk and egg proteins are hydrophilic and hence more soluble (Day & Cakebread, 2022).

The solubility of proteins is key in several functional properties, such as emulsification, foaming, gelling, and water absorption capacity (Kutzli et al., 2021; Li et al., 2013). Due to the low solubility of pulse proteins, their use in food products is challenging, hence physical, chemical, and/or biochemical modifications are needed to improve their functionality. Additionally, pulses have undesirable flavours. Harsh pH conditions used during pulse protein extraction can also cause structural changes (Sari et al., 2015). Physical treatments, such as heating, can denature the proteins and expose the hydrophobic residues that are usually within the core of the protein structure.

Pulse proteins can be made more hydrophilic by changing the pH and net charge or forming conjugates with hydrophilic compounds, such as

\* Corresponding author.

E-mail address: [edoardo.capuano@wur.nl](mailto:edoardo.capuano@wur.nl) (E. Capuano).

<https://doi.org/10.1016/j.jff.2023.105667>

Received 3 May 2023; Received in revised form 20 June 2023; Accepted 1 July 2023

Available online 6 July 2023

1756-4646/© 2023 The Authors. Published by Elsevier Ltd. This is an open access article under the CC BY license (<http://creativecommons.org/licenses/by/4.0/>).

sugars and polysaccharides. Glycation has proven effective in improving the functional properties of plant proteins, since the amino group side chains of the proteins bind to the reactive sides of the sugars to produce hydrophilic products (Li et al., 2013; Zha, Dong, et al., 2019; Zha, Yang, et al., 2019). Glycation of the proteins occurs in the initial stage of Maillard reaction to produce intermediate Amadori products, and advances further to produce melanoidins as end products. Melanoidins are brownish nitrogenous polymers (Kutzli et al., 2021; Martins et al., 2000). Previous reports show that the effect of glycation on the functional properties of the proteins depends on the extent or stage of Maillard reaction. The early stage enhances the functional properties of the proteins, whereas advanced glycation yields protein cross-linkages, off-flavours, and reduced digestibility (Kutzli et al., 2021; Zha, Yang, et al., 2019).

Glycation in foods can progress to the advanced stage of the Maillard reaction, where irreversible structural modification of the protein occurs, hence affecting protein digestibility (van der Lugt et al., 2020; Yang et al., 2022). After protein hydrolysis in the small intestine, partially hydrolysed and unabsorbed polypeptides move to the colon, where they can interact with the microbiota. If the proteins are modified, their digestibility and the nature of hydrolysates that reach the colon can be affected (Yang et al., 2022). Additionally, this change can influence the metabolites and population profile of the gut microbiota (van der Lugt et al., 2020; Yang et al., 2022). Dominika et al. reported higher abundance of commensal bacteria when the gut microbiota was exposed to glycated pea proteins compared to non-glycated proteins, whereas levels of short- and branched-chain fatty acids produced were not significantly different (Dominika et al., 2011).

Maillard reaction is common in processed foods with high protein content, whether animal sourced or plant-based, yet the effect of glycation on behaviour of proteins along the gastro-intestinal tract has not been extensively studied. This gap in literature is particularly notable for plant proteins. This study therefore aimed to evaluate the impact of glycation on the digestibility of lentil proteins as a model plant protein. Additionally, we studied the effect that the insoluble fraction of glycated lentil protein hydrolysates that potentially reach the colon has on gut microbiota metabolites and population, using batch fermentation and the Simulator of Human Intestinal Microbiome Ecosystem (SHIME®).

## 2. Materials & methods

### 2.1. Materials

Dry green lentils (*Lens culinaris*) were purchased from a local grocery store in Wageningen, Netherlands. D-Fructose was purchased from Merck Life Science NV, Netherlands. Pepsin (from porcine gastric mucosa,  $\geq 250$  units/mg solid), pancreatin (from porcine pancreas,  $8 \times$  USP specification), and bile extract (from porcine) were purchased from Merck Life Science NV, Netherlands. NuPAGE® LDS Sample buffer (4X), NuPAGE® SDS Running Buffer (20 $\times$ ), and NuPAGE®12 % Bis-Tris Gel (1.0 mm, 10 Well) were purchased from ThermoFisher Scientific, Netherlands. Coomassie Brilliant Blue R-250 Staining Solution was purchased from Merck Life Science NV, Netherlands. BlueRay Pre-stained Protein Marker 10–180 kDa was purchased from Jena Bioscience GmbH, Germany. Ammonia Assay Kit (Rapid) was purchased from Megazyme Ltd, Netherlands.

### 2.2. Lentil protein extraction

Green lentil seeds were soaked in water (1:3 w/v) at 20 °C overnight, freeze-dried, and milled into fine powder using a food processor. The flour was suspended in 0.05 M NaOH (10 %, w/v), and pH was adjusted to 10 to solubilize the proteins. The suspension was stirred constantly for 4 h and then centrifuged at 7000 g for 30 min at 20 °C. The solubilized proteins in the supernatant were precipitated by adjusting pH of the supernatant to 4 and stirring for 2 h. pH was adjusted using 3 M HCl and

3 M NaOH. Afterwards, the suspension was centrifuged at 7000 g for 30 min at 20 °C. The extracted lentil proteins (LP) were recovered as pellets and lyophilized. Prior to lyophilization, the pH was adjusted to 7. The protein content of LP was  $67.67 \pm 0.20$  %, as determined by the Dumas method. The nitrogen: protein conversion factor of 5.5 was used as suggested by Mossé (Mossé, 1990).

### 2.3. Glycation of lentil proteins

LP and D-fructose stock solutions (5 % w/v) were prepared in deionized water. Equal volumes of LPI and fructose stock solutions were mixed and lyophilized. The dry LP-fructose powder samples were incubated at 60 °C in a desiccator with a relative humidity of 79 % (Feng & Berton-Carabin et al., 2021). Relative humidity was achieved by adding saturated potassium bromide solution to the desiccator. The samples were incubated for 0, 24, and 48 h and hereafter referred to as LP+Fr0, LP+Fr1, and LP+Fr2, respectively. After incubation, samples were stored at  $-20$  °C until subsequent analysis.

### 2.4. Determination of particle size distribution

The particle size distribution of the glycated and non-glycated proteins were determined by dynamic light scattering using a Zetasizer Ultra (Malvern Panalytical Ltd., Worcestershire, UK). Sample solutions containing 1 mg/mL protein were prepared in Milli-Q water. A disposable cuvette was filled with a 1 mL aliquot and inserted in the Zetasizer for the particle size measurement. Duplicate measurements were performed for each sample.

### 2.5. Evaluation of molecular weight profile of glycated proteins by sodium dodecyl sulfate polyacrylamide gel electrophoresis (SDS-PAGE)

The molecular weight profile of the glycated and non-glycated LPs were evaluated by SDS-PAGE according to the NuPAGE® electrophoresis system manufacturer's instruction. First, 2  $\mu$ L of LP, LP+Fr0, LP+Fr1, and LP+Fr2 (with protein concentration of 0.5–1 mg/mL) were mixed with 5  $\mu$ L of LDS sample buffer and 15  $\mu$ L MilliQ water. The mixture was centrifuged for 1 min at 20 °C, 2000 rpm. Thereafter, the samples were incubated at 70 °C for 10 min and spun again at 2000 rpm and 20 °C for 1 min. The protein marker (5  $\mu$ L) and samples (10  $\mu$ L) were loaded onto the gel wells. The electrophoresis was run at 200 V for 35 min. The gel was then gently rinsed with water and stained with Coomassie Brilliant Blue R-250 Staining Solution for 1 h at 20 °C. Destaining was performed overnight with a washing buffer (containing 10 % ethanol, 7.5 % acetic acid, and Milli Q water) until the background colour of the gel was removed. The gel was then imaged.

### 2.6. Determination of Maillard reaction markers by LC-MS/MS

The levels of furosine, N $\epsilon$ -(carboxymethyl)-L-lysine (CML), and N $\epsilon$ -(carboxyethyl)-L-lysine (CEL) were determined using a high-pressure liquid chromatograph (HPLC) (Ultimate 3000, Thermo Scientific, USA). The HPLC was coupled with a TSQ Quantum triple quadrupole mass spectrometer (Thermo Finnigan, San Jose, CA, USA). Prior to sample loading, 200  $\mu$ L of 5 mg/mL of LP, LP+Fr0, LP+Fr1, and LP+Fr2 were hydrolysed under a fume hood in a capped heating tube containing 4 mL 6 M HCl. The headspace of the tubes was saturated with nitrogen to limit oxidation. The tubes were incubated at 110 °C for 22 h. After incubation, the sample was filtered with 0.2  $\mu$ m PTFE filters, and 500  $\mu$ L of the filtrate was transferred to an Eppendorf tube and dried completely with nitrogen gas. The dried samples were reconstituted in 490  $\mu$ L of Milli Q water and mixed with 10  $\mu$ L of internal standard mix to reach 25 ppm of d $_4$ -Fur, d $_4$ -CML and d $_4$ -CEL (Troise et al., 2015). Solid-phase extraction was performed, as previously described (Delatour et al., 2009). The elutes were evaporated at 35 °C and reconstituted in 200  $\mu$ L 50 % acetonitrile. The solution was centrifuged at 800 g and 20 °C for 1

min. The supernatant was transferred into a vial, and 10  $\mu$ L was loaded into the LCMS/MS system, as previously reported (Feng & Berton-Carabin et al., 2021). A reversed-phase core shell HPLC column was used for separation. The levels of furosine, CML, and CEL were determined using a calibration curve of known concentrations (0.025–10 ppm) standard against the corrected area (analyte peak area/internal standard peak area) (Feng & Berton-Carabin et al., 2021; Troise et al., 2015).

### 2.7. Simulated *in vitro* gastrointestinal digestion

LP and glycosylated LP samples were subjected to the COST INFOGEST method of simulated static *in vitro* gastrointestinal digestion (Minekus et al., 2014). In the oral phase, each 5 g of LP and glycosylated LP samples was mixed with 3.5 mL of simulated salivary fluid, 25  $\mu$ L of 0.3 M CaCl<sub>2</sub>, and 1.475 mL of MilliQ water. The mixture was incubated at 37 °C for 2 min. Thereafter, the bolus (10 mL) was mixed with 7.5 mL simulated gastric fluid, and pH was adjusted to 3 using 1 M HCl. A 1.6 mL aliquot of pepsin stock solution (25000 U/mL) was added to reach a concentration of 2000 U/mL. Additionally, 5  $\mu$ L of 0.3 M CaCl<sub>2</sub> was added. The final volume of the bolus was adjusted to 20 mL using MilliQ water and incubated at 37 °C for 2 h with constant shaking. After the gastric phase, the pH was adjusted to 7 using 1 M NaOH. For the intestinal phase, 11 mL of simulated intestinal fluid and 40  $\mu$ L of 0.3 M CaCl<sub>2</sub> were mixed with the gastric chyme. Additionally, 2.5 mL of fresh bile stock solution and 5 mL of pancreatin stock solution were added to the chyme. The final concentrations of bile and pancreatin in the chyme were 10 mM and 100 U/mL (based on trypsin activity), respectively. The volume of the intestinal chyme was adjusted to 40 mL using MilliQ water and incubated for 2 h at 37 °C with constant shaking. At the end of the intestinal phase, the digesta were immediately stored in a –20 °C freezer to halt enzymatic activities.

### 2.8. Determination of degree of hydrolysis (DH)

The degree of hydrolysis after the intestinal phase of *in vitro* digestion was determined using the *o*-phthalaldehyde (OPA) method (Nielsen et al., 2001). First, the OPA reagent was prepared by adding 3.81 g sodium tetraborate to a flask containing 80 mL Milli Q water. Subsequently, 0.088 g dithiothreitol, 0.1 g sodium dodecyl sulphate, and 0.080 g OPA dissolved in 2 mL ethanol were added to the solution. Milli Q water was further added to the flask, to reach a volume of 100 mL. L-serine (0.15–0.0125 mg/mL) was prepared and used for a standard curve. A 400- $\mu$ L aliquot of the standard, blank (Milli Q water), or digested samples were added to 3 mL of the OPA reagent, mixed for 5 s, and incubated at room temperature for 2 min. The absorbance of the resulting solution was measured at 340 nm using a spectrophotometer (Varian Cary® 50 UV–Vis, Spectralab Scientific Inc., Markham, Canada). DH was then determined as free amino groups from digestion/free amino groups from acid hydrolysis and expressed as a percentage. Acid hydrolysis was performed by mixing 5 g of samples (LP, LP+Fr0, LP+Fr1, and LP+Fr2) with 40 mL of 6 M HCl and incubating at 100 °C for 24 h.

### 2.9. Acid precipitation of digesta

Digested samples were subjected to acid precipitation to obtain the high molecular weight peptides as previously reported (Boachie et al., 2022). The pH of LP+Fr0, LP+Fr1, and LP+Fr2 digesta were adjusted to 4 under constant stirring for 30 min. The suspension was then centrifuged for 30 min at 7000 g and 20 °C. The sediment (recovered as insoluble and high molecular weight peptides) was freeze-dried. The recovered insoluble high molecular weight hydrolysates of LP+Fr0, LP+Fr1, and LP+Fr2 are hereafter referred to as LP+Fr0-H, LP+Fr1-H, and LP+Fr2-H, respectively.

### 2.10. Batch fermentation

The high molecular weight hydrolysates from the glycosylated LPs (LP+Fr0-H, LP+Fr1-H, and LP+Fr2-H) were used in a batch fermentation set-up to evaluate their effect on the metabolism of gut microbiota (Koper et al., 2019). Buffered colon medium was prepared with 5.22 g K<sub>2</sub>HPO<sub>4</sub>, 16.32 g KH<sub>2</sub>PO<sub>4</sub>, 2 g NaHCO<sub>3</sub>, 2 g yeast extract, 2 g peptone, 1 g mucin, 0.5 g L-cysteine HCl, and 2 mL Tween-80 in 1 L deionized water. A phosphate buffer was prepared with 8.8 g K<sub>2</sub>HPO<sub>4</sub>, 6.8 g, 0.1 g KH<sub>2</sub>PO<sub>4</sub>, and 0.1 g sodium thioglycolate in 1 L of deionized water. The medium, phosphate buffer, and 100 mL penicillin bottles and their caps were sterilized before use.

**Preparation of faecal inoculum:** Faecal samples were donated by three non-smoking healthy donors after giving their informed consent. Healthy volunteers gave written consent for a single faecal donation and their anonymity was granted at all times. According to the guidelines of the Medical Ethical Advisory Committee of Wageningen University (METC-WU), this research did not need ethical approval.

The donors had normal body mass indices and no recent histories of antibiotic use. The faecal inoculum was prepared by mixing fresh faecal samples with phosphate buffer at 200 mg/mL in a stomacher bag. The mixture was homogenized with a mixer for 10 min at 300 rpm. The suspension was centrifuged at 500 g for 2 min at 20 °C. The supernatant was recovered as the faecal inoculum. The faecal inoculum was prepared in a biosafety cabinet.

Thereafter, 21.5 mL medium and 10 mL sterile deionized water were added to the penicillin bottles and tightly closed with rubber caps and aluminium (Van Den Abbeele et al., 2018). LP+Fr0-H, LP+Fr1-H, and LP+Fr2-H were added to reach a concentration of 1 % w/v. Phosphate buffer was used as control. The bottles were flushed with nitrogen gas for 30 min to initiate anaerobic conditions. The faecal inoculum (3.5 mL) was added to the penicillin bottles. The bottles were incubated at 37 °C under mild rotation for 48 h. The samples were obtained at 0, 6, 24, and 48 h for further analysis of microbial metabolites.

### 2.11. Simulator of the human intestinal microbial ecosystem (SHIME®)

From the levels of metabolites obtained from the batch fermentation, LP+Fr0-H and LP+Fr2-H were selected to evaluate the effect of partially digested glycosylated LPs in the proximal and distal colon. The SHIME® system (PRODIGEST, Belgium) was used to simulate the colon, as previously described (Rovalino-Córdova et al., 2020). Briefly, the triple SHIME® comprising two connected double jacketed vessels was used to simulate the proximal and distal colon. Three sets of PC and DC vessels were used for the basal medium (as control), LP+Fr0-H, and LP+Fr2-H.

Faecal samples were provided by two non-smoking adult donors after giving their informed consent. Both donors had no history of probiotic or antibiotic use over the previous 6 months and no history of irritable bowel syndrome. Faecal inoculum was prepared as previously reported, fed to the SHIME to stabilize the microbial community for two weeks, and stored at –80 °C until further use (Rovalino-Córdova et al., 2020). The pre-stabilized faecal inocula was adapted to the SHIME® basal medium for 3 days before treatments were added. The basal medium comprised 1.2 g/L arabinogalactan, 2.0 g/L pectin, 0.5 g/L xylan, 0.4 g/L glucose, 3.0 g/L yeast extract, 1.0 g/L peptone, 3.0 g/L mucin, 0.5 g/L L-cysteine-HCl, and 4.0 g/L starch. PC vessels contained 500 mL at pH 5.6–5.9, and DC vessels contained 800 mL at pH 6.6–6.9 (Koper et al., 2019). During the adaptation period, 140 mL of basal medium was added to the vessels every 8 h. After the adaptation, the treatment period of 10 days was initiated. Growth media for the treatments were prepared by replacing 2.5 g/L starch in the basal medium with 2.5 g/L of either LP+Fr0-H or LP+Fr2-H. Every 8 h, 140 mL of growth medium was added to the system. Samples were taken on day 0, 1, 2, 3, 4, 7, 8, 9, and 10 at same time of the day. The aliquots were centrifuged at 9000 g, 4 °C for 5 min. Supernatants and pellets were stored separately at –20 °C until further analysis. The system was flushed with nitrogen daily to maintain

anaerobic conditions while running.

### 2.12. Determination of levels of short- and branched-chain fatty acids produced

Levels of short- and branched-chain fatty acids produced during *in vitro* fermentation of LP+Fr0-H, LP+Fr1-H, and LP+Fr2-H were evaluated as previously reported (Rovalino-Córdova et al., 2020). Supernatants obtained from fermentation were filtered using 15 mm of 0.2 µm RC filters. Calibration standard solutions (10–750 ppm) of acetic acid, propionic acid, butyric acid, valeric acid, isobutyric acid, and isovaleric acid were prepared. The internal standard containing 0.45 mg/mL of 2-ethylbutyric acid (in 0.3 M HCl and 0.9 M oxalic acid) was used. The filtered samples (100 µL) were mixed with 50 µL of internal standard in vials. The levels of short chain fatty acids in the samples were measured using the GC-2014 gas chromatograph (Shimadzu Corporation, Kyoto, Japan) coupled with a flame-ionization gas detector (FID). Additionally, 1 µL of the mixture was injected into a capillary fatty acid-free Stabil wax-DA column (1 µm × 0.32 mm × 30 m) (Restek, Bellefonte, PA, USA).

### 2.13. Determination of levels of ammonia produced

Levels of ammonia produced were measured according to the microplate assay procedure provided by the Ammonia Assay Kit (Rapid) purchased from Megazyme Ltd, Netherlands.

Briefly, 210 µL of distilled water, 30 µL of assay buffer, and 20 µL of NADPH solution were added to blank wells. To the sample and standard wells, 10 µL of sample (supernatants obtained from fermentation) or standard, 200 µL of distilled water, 30 µL of assay buffer, and 20 µL of NADPH were added. The plates were mildly shaken to mix the solutions in the wells and incubated for 2 min. The absorbance at 340 nm was read after the initial incubation. Glutamate dehydrogenase solution (2 µL) was added to each well and incubated again for 5 min. The final absorbance was read at 340 nm. Ammonia levels present were calculated as indicated in the manufacturer's manual.

### 2.14. Determination of population profile

DNA was isolated from pellets obtained from the SHIME® samples using QIAamp PowerFecal Pro DNA Kit (Qiagen Inc., Hilden, Germany). The yield was quantified using Qubit HS Fluorescence (Invitrogen, Waltham, USA). Afterwards, 2.5 µL of the DNA material was used to amplify bacterial 16S rRNA gene variable V3 and V4 regions by polymerase chain reaction. The primers, Pro341F CCTACGGGNGCASCAG and Pro805R GACTACNVGGGTATCTAATCC, were used with universal extension, as recommended by the 16S Metagenomic Sequencing Library Preparation guidelines from Illumina (San Diego, USA). After initial amplification of the 16S target region, amplicons were purified and analysed on a Bioanalyzer with DNA1000 chips. Indexing PCR was performed using Nextera UD index adapters from Illumina (San Diego, USA). Barcoded amplicons were quantified using Qubit HS Fluorescence and the equimolar pooled. Sequencing was performed on the Illumina MiSeq instrument using v2 flow cell and chemistry with 4 pM library loading concentration. Paired end reads sequencing was obtained by 2 \* 251 cycles. Base calling and subsequent data demultiplexing were performed using bcl2fastq v2.20.0.422. The Qiime2 platform (<https://qiime2.org>) was used to identify and classify taxonomic units (Bolyen et al., 2019). Diversity analyses were performed using the qiime2 diversity tool.

### 2.15. Statistical analysis

Mean ± standard deviation of triplicate particle size, furosine, and CEL measurements of glycosylated lentil proteins were reported. The mean ± standard deviation of biological triplicate measurements of *in vitro*

protein degree of hydrolysis, ammonia, short- and branched-chain fatty acids were reported. Repeated measure analysis of variance (two-way) with Tukey post hoc test was used to determine significant differences between mean values at  $P < 0.05$ .

## 3. Results & discussion

### 3.1. Particle size of glycosylated and non-glycosylated proteins

The average particle sizes of the native protein and glycosylated samples were measured to determine possible modification of their particle characteristics. Compared to the particle size of LPs, the particle size of the glycosylated samples increased as incubation time increased (Fig. 1A). The highest increase occurred in LP+Fr2, where the average particle size was about twice that of LP particles. LP+Fr0 particles were comparable to those of LP. Considering the similarity in particle size of LP and LP+Fr0, the presence of fructose residues did not significantly influence the size of the proteins as much as the incubation temperature. The observed increase in LP+Fr1 and LP+Fr2 were likely due to aggregation from the incubation temperature of 60 °C. This was further confirmed by the increase in average particle size as incubation time increased.

Feng et al. reported that due to aggregation, soy protein-glucose conjugates had larger particles than the unheated soy protein-glucose conjugates (Feng & Berton-Carabin et al., 2021). In another study, Yang et al. measured absorbance as an indicator of protein aggregation and observed that absorbance of ovalbumin-glucose conjugates decreased as degree of glycation increased (Yang et al., 2022). Wang et al. also observed that the particle size of egg white-isomaltooligosaccharide conjugates were larger than that of the native egg protein due to aggregation. However, the hydrodynamic diameter of conjugates was smaller than that of the native protein due to high electrostatic repulsion within the egg native protein (Wang et al., 2019). The molecular weight range, hydrophilicity, and solubility of the proteins tend to favour the trend observed by Wang et al.

### 3.2. Maillard reaction markers

Condensation between the amino side chain of proteins and carbonyl group of reducing sugars forms Amadori products at the initial stage of the Maillard reaction. Acid hydrolysis of these products produces furosine which is then used as an indicator of the early stage of the Maillard reaction. CML and CEL are formed during the advanced stages of the reaction (Cui et al., 2021; Feng & Berton-Carabin et al., 2021). Therefore furosine, CML, and CEL were measured as indicators of the extent of Maillard reaction in the glycosylated LP samples.

The levels of furosine increased as incubation time increased, such that levels recorded in LP+Fr1 and LP+Fr2 were 30 times and 70 times higher than that of LP, respectively (Fig. 1C). About a two-fold increase was observed from 24 h incubation to 48 h incubation, confirming that glycation of proteins is dependent on time and temperature of incubation. The levels of CEL in LP+Fr1 and LP+Fr2 were about 5 times and 10 times that of LPI, respectively (Fig. 1D). Therefore, doubling the incubation time produced a two-fold increase in CEL levels, as observed in LP+Fr1 and LP+Fr2. CML levels were below detectable limits.

During the early stage of Maillard reaction, the electrophilic carbonyl carbon of a reducing sugar binds to a free non-protonated amino group, such as ε-amino group of lysine, to form an imine. The imine, also known as Schiff's base, rearranges into more stable products known as Amadori or Heyns products, if the carbonyl group is from an aldose or ketose, respectively (Wrodnigg & Eder, 2001). Furosine [ε-N-(furoylmethyl)-l-lysine] is an example of these stable products formed. After protein glycation in the early stage of the Maillard reaction, several reactions, including degradation, dehydration, and fission reactions, transform the stable Amadori/Heyns products into reactive compounds that further degrade, cyclise, enolise, oxidise, or rearrange to produce advanced glycation products (Inan-Eroglu et al., 2020; Zhang et al.,

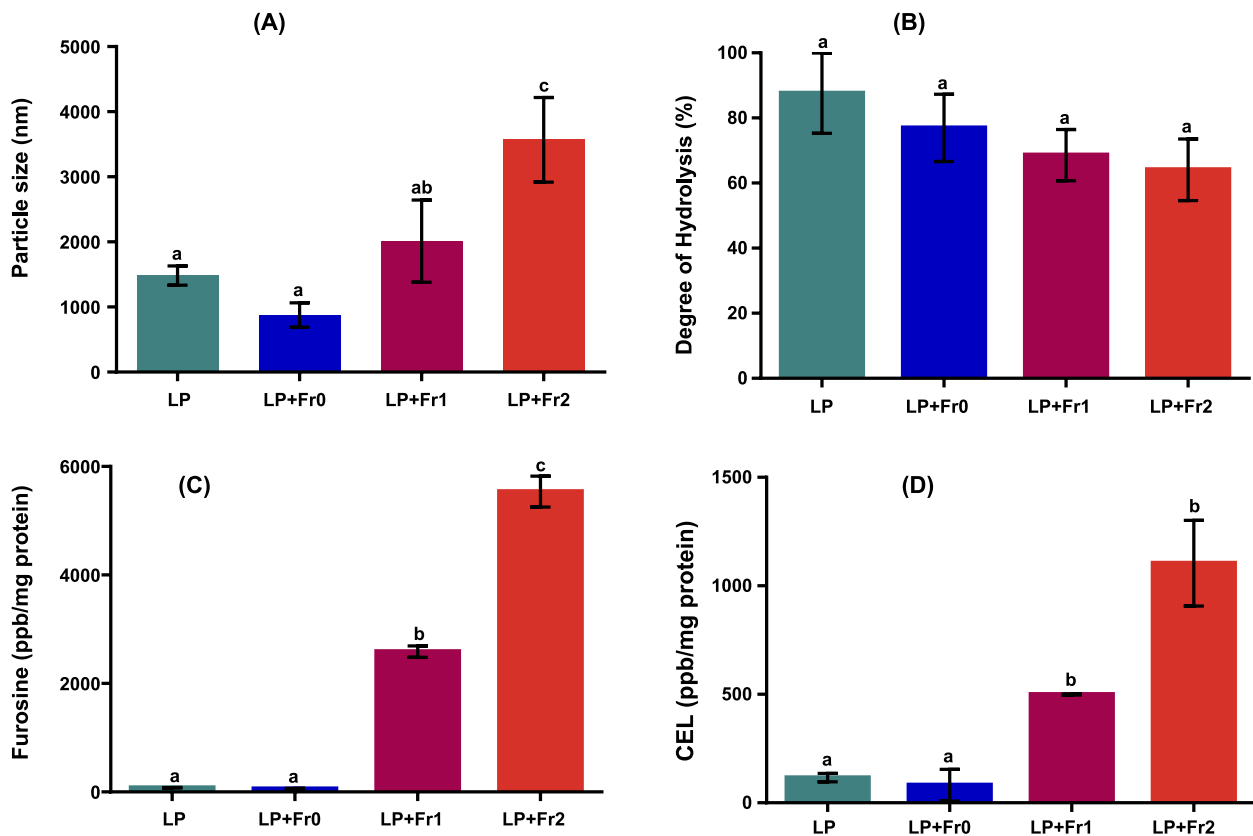


Fig. 1. (A): Particle size of lentil protein and lentil protein-fructose conjugates (B): Degree of hydrolysis (%) of lentil protein-fructose conjugates after simulated *in vitro* gastrointestinal digestion (C): Levels of furosine in lentil protein-fructose conjugates (D): Levels of CEL in lentil protein-fructose conjugates. Conjugates were prepared with dry lentil protein + fructose (1:1) mixture incubated at 60 °C for 0, 24, or 48 h (referred to as LP+Fr0, LP+Fr1, and LP+Fr2). Different letters represent statistically significant differences ( $P < 0.05$ ).

2011). CEL is from methylglyoxal and lysine and can be used as an indicator of the advanced stage of the Maillard reaction (Kutzli et al., 2021).

The extent of the Maillard reaction depends on several factors, including water activity, molecular weight, pH, temperature, and incubation time (de Oliveira et al., 2016; Feng & Berton-Carabin et al., 2021). Our results show that the levels of Maillard reaction products can correspondingly increase with incubation time. Increasing the heating time allows for more interaction between the reducing sugar and free amino group. Moreover, considering the globular structure of the predominant proteins in lentils, heating can unfold the proteins, expose the reactive amino groups, and speed up conjugation. The onset temperature of thermal denaturation of lentil proteins have been reported to occur around 70 °C and peak around 80 °C (Barbana & Boye, 2013). The reactive form of sugars, which is the open chain form, also increases at high temperatures (Van Boekel, 2001; Wu et al., 2020). The unfolding effect of heat is confirmed by the comparable levels of furosine and CEL in LP and LP+Fr0. These samples were not exposed to heat as the other samples. Additionally, the pH of all the samples was neutral (pH 7); hence, both the carbonyl groups and free amino groups existed in their reactive forms. The neutral pH eliminates the possible marked contribution from different pH conditions in samples. Feng et al. also observed a substantial increase in furosine and CEL levels in a soy protein-glucose system produced under similar conditions as the present study (Feng & Berton-Carabin et al., 2021).

### 3.3. Degree of protein hydrolysis after simulated *in vitro* gastrointestinal digestion

The extent of hydrolysis after digestion was measured by

determining the fraction of amino groups that has been cleaved from the protein backbone. The DH of LP was the highest (87.62 %  $\pm$  12.33), followed by LP+Fr0. The lowest was observed in LP+Fr2, with DH of 64.10 %  $\pm$  9.44. DH decreased as the incubation period increased, although without statistical significance. The increase in particle size of LP+Fr1 and LP+Fr2 and the corresponding decrease in their DH suggest that aggregation contributed to the decrease in digestibility.

From our results, the presence of fructose slightly reduced the DH after *in vitro* digestion. Condensation reactions that occur during glycation, even at the initial stage of the Maillard reactions, involve covalent interactions and cross-linkages that yield products that are less susceptible to proteases (Xu et al., 2020; Zhang yao et al., 2023). The structural change around the reacting amino group likely reduces the proteins' susceptibility to proteases in the pancreatin used in the intestinal phase. For instance, trypsin is known to cleave the carboxyl end of lysine and arginine. However, the  $\epsilon$ -amino groups of lysine are known as the main amino groups involved in the Maillard reaction amongst others, such as the guanidine group in arginine, imidazole in histidine, and indole from tryptophan (de Oliveira et al., 2016). Additionally, leguminous proteins have high levels of arginine and lysine. Hence, glycation at the lysine residues can decrease the digestibility of the glycated samples. Although the possible mechanism by which digestibility was reduced in our study was not evaluated, it is likely that access of proteases to peptide bonds was reduced by modification of cleavage sites involving carboxyl groups of lysine and arginine, and steric hindrance caused by the condensation and crosslinking reactions. Glycation has been reported to reduce digestibility of casein and ovalbumin such that ovalbumin's digestibility decreased proportionally to the extent of glycation (Yang et al., 2022; Zhao et al., 2017).

DH in the heat-incubated samples (LP+Fr1 and LP+Fr2) were

slightly lower than the levels in the unheated samples (LP and LP+Fr0). High temperatures have been reported to enhance the rate of the Maillard reaction to produce more digestion-resistant end products. The reactive open form of sugars commonly occurs at high temperatures, and globular proteins also unfold at elevated temperatures. The incubation temperature (60 °C) used in our study is slightly below the onset temperature of thermal denaturation reported in literature (~70 °C) (Barbana & Boye, 2013), however it is likely that unfolding of the globular proteins was initiated during the 24-h and 48-h incubation period, and thus proteins were slightly unfolded. Therefore, the decreased DH in the heated samples could be due to the presence of more Maillard reaction products and possible aggregation at the incubation temperature.

### 3.4. Molecular weight profile of glycosylated and non-glycosylated proteins by SDS-PAGE

The molecular weight profile of LP shows bands at 17–100 kDa (Fig. 2A). Bands observed around 25 kDa and 48 kDa correspond to basic and acidic subunits of legumin, respectively. The band that is slightly above 63 kDa corresponds to vicilin trimers held by hydrophobic interactions. Convicilin was observed around 75–100 kDa (Shevkani et al., 2019). The profile of LP+Fr0 was comparable to that of LP. LP+Fr0 was mixed with fructose but was not heated. However, after incubating at 60 °C for 24 h and 48 h, predominant bands corresponding to 63–75 kDa were faint in LP+Fr1 and even fainter in LP+Fr2. The incubation of these large proteins likely caused the globular structure to unfold and expose the reactive sites for glycation. The glycation likely progressed to the advanced stages to produce large MRPs that do not bind to SDS nor migrate through the gel, hence the reduced intensity of the bands. Comparably, disappearance of bands in a pea protein-gum arabic complex has been reported (Zha, Yang, et al., 2019). Bands for the low molecular weight proteins (17–25 kDa) in LP+Fr1 and LP+Fr2 almost disappeared. The decrease of the 17–25 kDa bands suggests that these low molecular weight proteins were likely involved in the condensation reaction between their free amino groups and the carbonyl groups of fructose.

Condensation between the proteins and fructose and the possible interprotein cross-linkages are expected to cause an increase in the molecular weight of the proteins. However, the advanced stage of the Maillard reaction involves complex reactions that can yield either low or high molecular weight products. The observed brown colour of the

glycosylated samples indicates the presence of melanoproteins which are formed by cross-linkage between proteins and MRPs (Feng, Berton-Carabin, Fogliano, & Schroën, 2022). Melanoidins can possess high molecular weights and low solubility; hence, it is likely that they did not migrate along the gel (Zha, Yang, et al., 2019). Overall, these results show that glycation modified the molecular weight profile of the proteins.

Digested LP (LP-dig) showed bands around 11 kDa, and these bands were not present in the undigested sample. Additionally, prominent bands were observed around 25 kDa and 63 kDa. The prominent bands at 63–75 kDa in the undigested sample disappeared after digestion. However, the only prominent band in the digested glycosylated samples (LP+Fr1 and LP+Fr2) was around 25 kDa and became fainter as incubation time increased.

### 3.5. Metabolites produced after batch fermentation of glycosylated and non-glycosylated lentil proteins

Insoluble high molecular weight hydrolysates from *in vitro* digestion of the glycosylated LPs (LP+Fr0, LP+Fr1, and LP+Fr2) were subjected to batch fermentation to evaluate how the extent of glycation affects metabolites produced by the gut microbiota. The insoluble hydrolysates were used as a representation of the fraction reaching the colon. Same amount of hydrolysates (1 % w/v) was added to the fermentation vessels irrespective of the extent of the glycation and degree of hydrolysis.

The levels of SCFAs and BCFAs produced from the glycosylated proteins over the 48-h fermentation period were comparable, except for the slight differences observed in propionic acid and butyric acid at 48 h (Table 1). Production of BCFAs evidently began after 6 h. BCFA production indicates that proteins are the only available carbon source in the substrate (Ashaolu et al., 2019; Neis et al., 2015). Carbohydrates are the primary and preferred substrate for the gut microbiota; therefore, when carbohydrates are available, protein fermentation is restricted. This confirms the relative delay in production of BCFAs until the carbohydrates in the medium were likely exhausted (see Table 1).

The levels of ammonia increased significantly at 6 h and 24 h, after which levels remained fairly constant (Table 2). The increase observed at 24 h was higher in LP+Fr0-H than in the other hydrolysates. Overall, the effect of time was statistically significant ( $P < 0.0001$ ), whereas the effect of treatment was not ( $P = 0.71$ ).

Dominika et al. observed a higher production of acetic acid after *in*

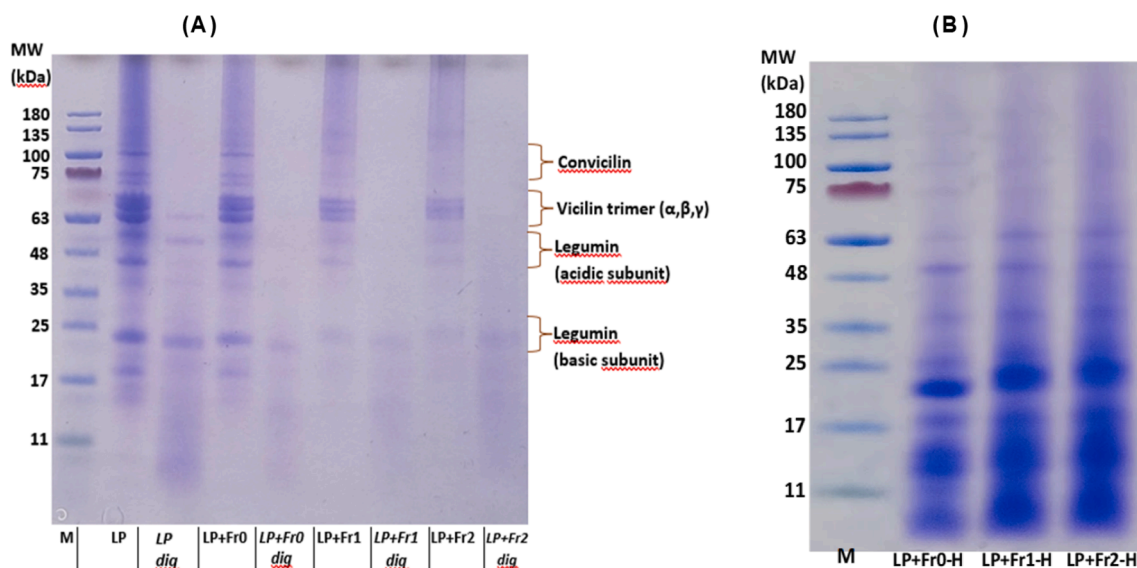


Fig. 2. Molecular weight (MW) profile of (A): non glycosylated lentil protein (LP), glycosylated lentil proteins (LP+Fr0, LP+Fr1, and LP+Fr2), and their digests (LP dig, LP+Fr0 dig, LP+Fr1 dig, and LP+Fr2 dig). (B): Insoluble hydrolysates obtained from acid precipitation of digested LP+Fr0, LP+Fr1, and LP+Fr2 labelled as LP+Fr0-H, LP+Fr1-H, and LP+Fr2-H. MW was evaluated with SDS-PAGE under non-reducing conditions.

**Table 1**

Increase in short- and branched-chain fatty acids recorded after supplementing growth medium with LP+Fr0-H, LP+Fr1-H, and LP+Fr2-H in a 48 h-batch fermentation.

Concentration (mM)	Time (h)	Control (Basal medium)	LP+Fr0-H	LP+Fr1-H	LP+Fr2-H
<b>Short-chain fatty acids</b>					
Acetic acid	6	2.41 ± 0.51 <sup>a</sup>	6.09 ± 1.93 <sup>a</sup>	5.56 ± 1.38 <sup>a</sup>	5.62 ± 1.44 <sup>a</sup>
	24	0.76 ± 0.74 <sup>a</sup>	7.31 ± 2.47 <sup>ab</sup>	6.87 ± 1.29 <sup>ab</sup>	6.89 ± 1.25 <sup>ab</sup>
	48	1.69 ± 0.60 <sup>a</sup>	10.14 ± 3.00 <sup>b</sup>	10.53 ± 2.36 <sup>b</sup>	10.93 ± 1.95 <sup>c</sup>
Propionic acid	6	0.34 ± 0.15 <sup>a</sup>	0.13 ± 0.08 <sup>a</sup>	0.16 ± 0.05 <sup>a</sup>	0.18 ± 0.11 <sup>a</sup>
	24	0.68 ± 0.19 <sup>a</sup>	3.53 ± 0.83 <sup>b</sup>	3.22 ± 0.39 <sup>b</sup>	2.98 ± 0.35 <sup>b</sup>
	48	0.46 ± 0.65 <sup>a</sup>	5.68 ± 1.68 <sup>b</sup>	5.33 ± 1.58 <sup>b</sup>	5.35 ± 1.01 <sup>b</sup>
Butyric acid	6	<0.01	<0.01	0.01 ± 0.01	0.01 ± 0.01 <sup>a</sup>
	24	0.01 ± 0.01 <sup>a</sup>	0.07 ± 0.11 <sup>a</sup>	0.05 ± 0.08 <sup>a</sup>	0.05 ± 0.08 <sup>a</sup>
	48	nd	0.50 ± 0.42 <sup>a</sup>	0.38 ± 0.63 <sup>a</sup>	0.59 ± 0.53 <sup>b</sup>
Valeric acid	6	nd	nd	Nd	nd
	24	nd	0.16 ± 0.28 <sup>a</sup>	0.12 ± 0.21 <sup>a</sup>	0.11 ± 0.20 <sup>a</sup>
	48	nd	0.70 ± 1.20 <sup>a</sup>	0.82 ± 1.42 <sup>a</sup>	0.81 ± 1.40 <sup>a</sup>
Total SCFA	6	2.75 ± 0.62 <sup>a</sup>	6.23 ± 2.01 <sup>a</sup>	5.72 ± 1.44 <sup>a</sup>	5.80 ± 1.56 <sup>a</sup>
	24	1.45 ± 0.92 <sup>a</sup>	11.07 ± 3.40 <sup>b</sup>	10.26 ± 1.70 <sup>b</sup>	10.03 ± 1.55 <sup>b</sup>
	48	2.00 ± 1.12 <sup>a</sup>	17.01 ± 3.23 <sup>c</sup>	15.29 ± 3.11 <sup>c</sup>	17.68 ± 1.08 <sup>c</sup>
<b>Branched-chain fatty acid</b>					
Isobutyric acid	6	nd	nd	nd	nd
	24	nd	nd	0.12 ± 0.20 <sup>a</sup>	0.10 ± 0.18 <sup>a</sup>
	48	nd	nd	0.46 ± 0.80 <sup>a</sup>	0.46 ± 0.80 <sup>a</sup>
Isovaleric acid	6	0.04 ± 0.07 <sup>a</sup>	nd	0.16 ± 0.28 <sup>a</sup>	nd
	24	0.07 ± 0.12 <sup>a</sup>	0.57 ± 0.90 <sup>a</sup>	0.62 ± 0.52 <sup>a</sup>	0.47 ± 0.55 <sup>a</sup>
	48	0.38 ± 0.67 <sup>a</sup>	1.48 ± 1.79 <sup>a</sup>	1.65 ± 2.23 <sup>a</sup>	1.73 ± 2.10 <sup>a</sup>
Total BCFA	6	0.04 ± 0.07 <sup>a</sup>	Nd	0.16 ± 0.28 <sup>a</sup>	Nd
	24	0.07 ± 0.12 <sup>a</sup>	0.57 ± 0.90 <sup>a</sup>	0.73 ± 0.72 <sup>a</sup>	0.57 ± 0.73 <sup>a</sup>
	48	0.38 ± 0.67 <sup>a</sup>	1.48 ± 1.78 <sup>a</sup>	2.12 ± 3.03 <sup>a</sup>	2.19 ± 2.89 <sup>a</sup>

LP+Fr0-H, LP+Fr1-H, and LP+Fr2-H are the insoluble hydrolysates obtained from acid precipitation of digested LP+Fr0, LP+Fr1, and LP+Fr2, respectively. Basal growth medium was used as control. Different superscripts indicate statistical difference ( $P < 0.05$ ) between hydrolysates at different timepoints. nd: not detected.

*in vitro* fermentation of non-glycated pea proteins than glycated pea proteins, although the difference was not statistically significant (Dominika et al., 2011). Yang et al. also recorded a higher production of acetate and propionate after *in vitro* fermentation of 24-h glycated fish protein hydrolysates (Yang et al., 2018). However, our results do not show any remarkable differences between the glycated and non-glycated proteins. This difference could be because we used the insoluble fraction after digestion, whereas these studies used the whole digests. The insoluble fractions were obtained as pellets from acid precipitation of the digested samples, mainly consisting of high molecular weight polypeptides. Proteolytic bacteria initially hydrolyse large peptides to produce free amino acids before subsequent catabolism into bacterial metabolites, unlike in the case of amino acids in the whole digests used in the other

**Table 2**

Increase in levels of ammonia produced after supplementing growth medium with LP+Fr0-H, LP+Fr1-H, and LP+Fr2-H in a 48 h-batch fermentation.

Time (h)	Concentration (mg/mL)			
	Control (basal medium)	LP+Fr0-H	LP+Fr1-H	LP+Fr2-H
6	15.28 ± 10.04 <sup>a</sup>	24.00 ± 12.58 <sup>a</sup>	20.56 ± 10.41 <sup>a</sup>	18.51 ± 9.91 <sup>a</sup>
24	28.68 ± 12.35 <sup>b</sup>	44.41 ± 11.94 <sup>b</sup>	31.44 ± 13.77 <sup>b</sup>	33.24 ± 4.98 <sup>b</sup>
48	30.72 ± 13.49 <sup>b</sup>	37.57 ± 13.77 <sup>b</sup>	36.40 ± 11.99 <sup>b</sup>	35.23 ± 15.28 <sup>b</sup>

LP+Fr0-H, LP+Fr1-H, and LP+Fr2-H are the insoluble hydrolysates obtained from acid precipitation of digested LP+Fr0, LP+Fr1, and LP+Fr2, respectively. Basal growth medium was used as control. Different superscripts indicate statistical difference ( $P < 0.05$ ) between hydrolysates at different timepoints.

studies (Diether & Willing, 2019).

Proteins can escape complete hydrolysis due to reduced access of the proteases. These undigested or partially digested peptides move to the large intestines where the microbiota can further metabolize them. Conversion of peptides to microbial metabolites involves microbial peptidase activity, deamination, and decarboxylation (Duncan et al., 2021). The predominant pathway involves deamination of the amino acids to produce SCFAs and ammonia. BCFAs are formed from deamination of branched-chain amino acids, such as leucine, isoleucine, and valine. The microbiota can also decarboxylate amino acids to produce amines and carbon dioxide (Oliphant & Allen-Vercocoe, 2019). Acetate can be produced from glutamate, glycine, proline, histidine, cysteine, and lysine. Propionate is mainly produced from aspartate and threonine, whereas butyrate can be formed from glutamate, alanine, methionine, and lysine. Butyrate can also be produced from glutamate, alanine, lysine, serine, and methionine (Fan et al., 2015). Considering that lysine and arginine can serve as substrates for SCFAs, condensation between these amino acid residues and reducing sugars can reduce levels of SCFAs produced from fermentation. However, our results do not confirm the hypothesis that LP+Fr2 should have low SCFA due to the extent of glycation. This finding is in line with recent studies showing that Maillard reaction products resist digestion, can be transported to the colon (van der Lugt et al., 2020), and are degraded within 24 h of fermentation (Hellwig et al., 2015). Additionally, Bui et al. reported that an isolated pure culture produced butyrate from N-ε-fructoselysine (Bui et al., 2015). This suggests that the Maillard reaction products in LP+Fr2 were fermented by the gut microbiota.

### 3.6. Population profile and diversity of the gut microbiota using the SHIME®

The effect of glycation of LPs on the population profile of the gut microbiota in the proximal and distal colon selections were evaluated by fermenting LP+Fr0-H and LP+Fr2-H for 10 days in the SHIME®. LP+Fr0-H and LP+Fr2-H were selected to evaluate the effect of extent of glycation, since no sizeable differences in metabolites were observed among LP+Fr0-H, LP+Fr1-H, and LP+Fr2-H. The richness and abundance of the population were evaluated by Alpha diversity based on phylogenetic diversity (Fig. 3A) and Beta diversity based on Bray-Curtis distance (Fig. 3B). No significant differences were observed between the diversity in the population from fermentation of LP+Fr0-H and LP+Fr2-H. However, notable differences were observed between the colon sections, such that the alpha diversity index of the proximal colon was lower than the median in both treatments and timepoints. Bray-Curtis distances also clustered based on the colon section (Fig. 3B). Firmicutes, Bacteroidetes, Proteobacteria, and Actinobacteria were the predominant phyla observed in all samples (Fig. 4A).

The relative abundance of Firmicutes reduced in both proximal and distal colon sections in Donor 1 (Table S1). The decrease, however, was

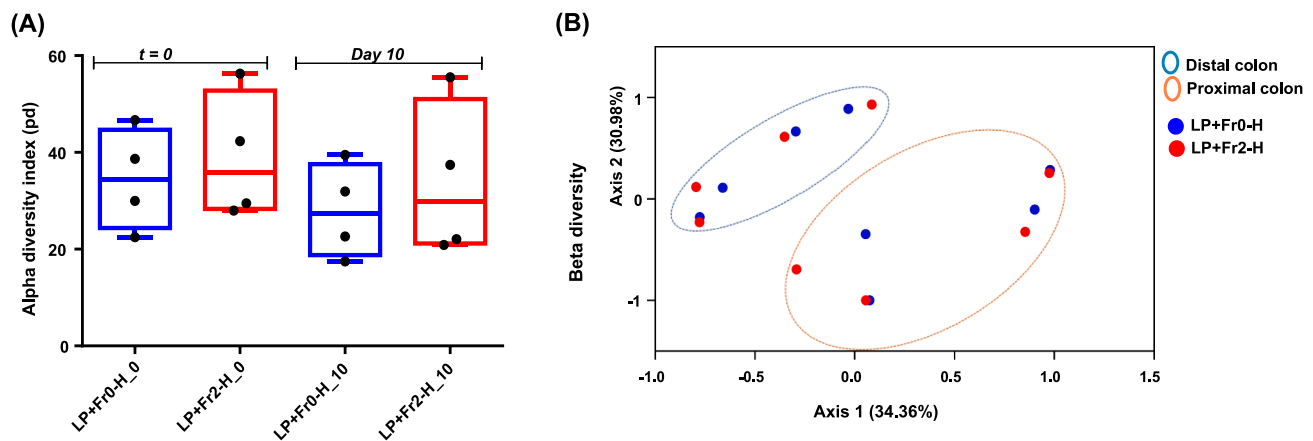


**Fig. 3.** Diversity measures from 16S rRNA gene sequencing results after supplementing growth medium with insoluble hydrolysates (LP+Fr0-H and LP+Fr2-H) in a 10 day-fermentation with SHIME®. (A): Alpha diversity based on phylogenetic diversity of microbial population (B): Beta diversity based on Bray-Curtis distance between treatments. LP+Fr0-H and LP+Fr2-H are the insoluble hydrolysates obtained from acid precipitation of digested LP+Fr0 and LP+Fr2, respectively. LP+Fr0-H\_0 are results from initial sampling (t = 0) whereas LP+Fr0-H\_10 are from final sampling (day10).

higher in the proximal section of LP+Fr2-H, with about 20 % relative decrease compared to about 3.7 % decrease observed in LP+Fr0-H. In the distal colon of Donor 2, slight increases were observed. LP+Fr0-H and LP+Fr2-H caused about 26 % and 42 % increase, respectively, in Bacteroidetes in the proximal colon of Donor 1. Firmicutes are known to preferably ferment oligosaccharides rather than peptides, hence the decrease observed (Tyakht et al., 2013). Although starch might be the primary and preferred substrate, peptides provide fermentable carbon substrates in the distal colon. The distal colon has low carbohydrate levels due to their depletion in the proximal colon (Peled & Livney, 2021; Taciak et al., 2017), hence the low abundance of Firmicutes. Consequently, the distal gut is colonized by amino acid fermenting groups, such as *Bacteroides*, *Clostridium*, *Fusobacterium*, *Streptococcus*, *Lactobacillus*, and *Peptococcus* spp. that hydrolyze peptides that reach the large intestine (Amaretti et al., 2019).

At the family level, *Bacteroidaceae* increased by about 25 % and 40 % in LP+Fr0-H and LP+Fr2-H, respectively (Fig. 4B). LP+Fr2-H seems to favour the growth of Bacteroidetes. The increase conforms to findings from Aguirre et al., where Bacteroidetes increased significantly during fermentation of a high-protein diet (Aguirre et al., 2016). Our results show that LP+Fr0-H and LP+Fr2-H differentially modulated the bacteria population profile in both colon sections depending on the donor. The differences observed after fermentation of LP+Fr0-H and LP+Fr2-H were mainly in the relative abundance of Firmicutes, Bacteroidetes, and Verrucomicrobia. Yang et al. observed a modulatory effect of glycated fish protein where relative abundance of Firmicutes and Bacteroidetes reduced compared to the non-glycated fish protein (Yang et al., 2018). This effect was attributed to higher levels of sugar substrates in the glycated proteins than in the native fish protein. Notably, Yang et al. fermented the whole digesta, whereas the insoluble undigested fraction (from acid precipitation) of the digesta was used in our study to mimic the fraction that reaches the colon. The main difference between LP+Fr0-H and LP+Fr2-H could be the type of peptides produced post-digestion due to the extent of glycation and the levels of Maillard reaction products. The SDS-PAGE showed that bands around 25 kDa were more prominent and slightly higher for LP+Fr2-H than the same bands in LP+Fr0-H (Fig. 2B).

Similar to the batch fermentation, no significant differences in the levels of SCFA, BCFA, and ammonia were observed between LP+Fr0-H and LP+Fr2-H (Figs. S1–S3 in Supplementary material). This suggests that either the substrates from these hydrolysates were similar and were catabolized similarly or the Maillard reaction products in LP+Fr2 were catabolized to produce SCFA, BCFA, and ammonia. The sugar residues were likely cleaved prior to bacterial proteolytic activity. Bui et al.

reported that isolated *Intestinimonas* strain AF211 is able to convert fructoselysine into butyrate (Bui et al., 2015). In another study by Borelli and Fogliano, *Bifidobacteria* recorded substantial proliferation compared to Clostridia, Streptococci, and Enterobacteriaceae when exposed to melanoidins. Although inconclusive, the authors suggest that Bifidobacteria use these melanoidins as source of carbon and nitrogen for their metabolism, hence the growth recorded (Borelli & Fogliano, 2005).

Considering the conditions used in the SHIME® fermentation set-up in this study, a growth medium that contains only glycated protein hydrolysates and no other source of nitrogen, such as peptone would have given further insights into the effect of glycation on gut microbiota metabolism and the population profile. This study supplemented the SHIME® growth media with glycated protein hydrolysates at a standardized concentration. The difference between *in vitro* protein digestibility of the LP+Fr0 and LP+Fr2 did not substantially influence the amount of insoluble pellets produced after digestion, thus, we mainly focused on how extent of protein glycation affected gut microbiota population profile and metabolites.

#### 4. Conclusion

In this study, we evaluated the effect of glycation on plant protein digestibility. We further studied the effect of glycated plant protein hydrolysates that might reach the colon on gut microbiota metabolites and population using batch fermentation and SHIME®. Lentil protein was selected as a model plant protein. As the incubation period of glycation increased, the digestibility decreased, though no statistical significance was recorded. A decrease in digestibility is mainly attributed to the aggregation of the proteins. The molecular weight profile was modified by glycation of the proteins. However, this modification in the protein profile did not cause a significant difference in the levels of metabolites produced during *in vitro* colonic fermentation. Additionally, no significant differences were observed in the diversity of the microbial population after a 10-day fermentation of the insoluble high molecular weight hydrolysates. The 16S rRNA gene sequencing showed that the hydrolysates differentially modulated donors' microbiota profile in the proximal and distal colon sections.

The main difference among the hydrolysates is the type of peptides produced post-digestion due to the extent of glycation and the amount of Maillard reaction products. Therefore, we postulate that on the one hand, the substrates from these hydrolysates are similar and catabolized similarly. On the other hand, the Maillard reaction products from the highly glycated proteins were also catabolized to produce SCFA, BCFA, and ammonia. Our findings show that the extent of glycation does not

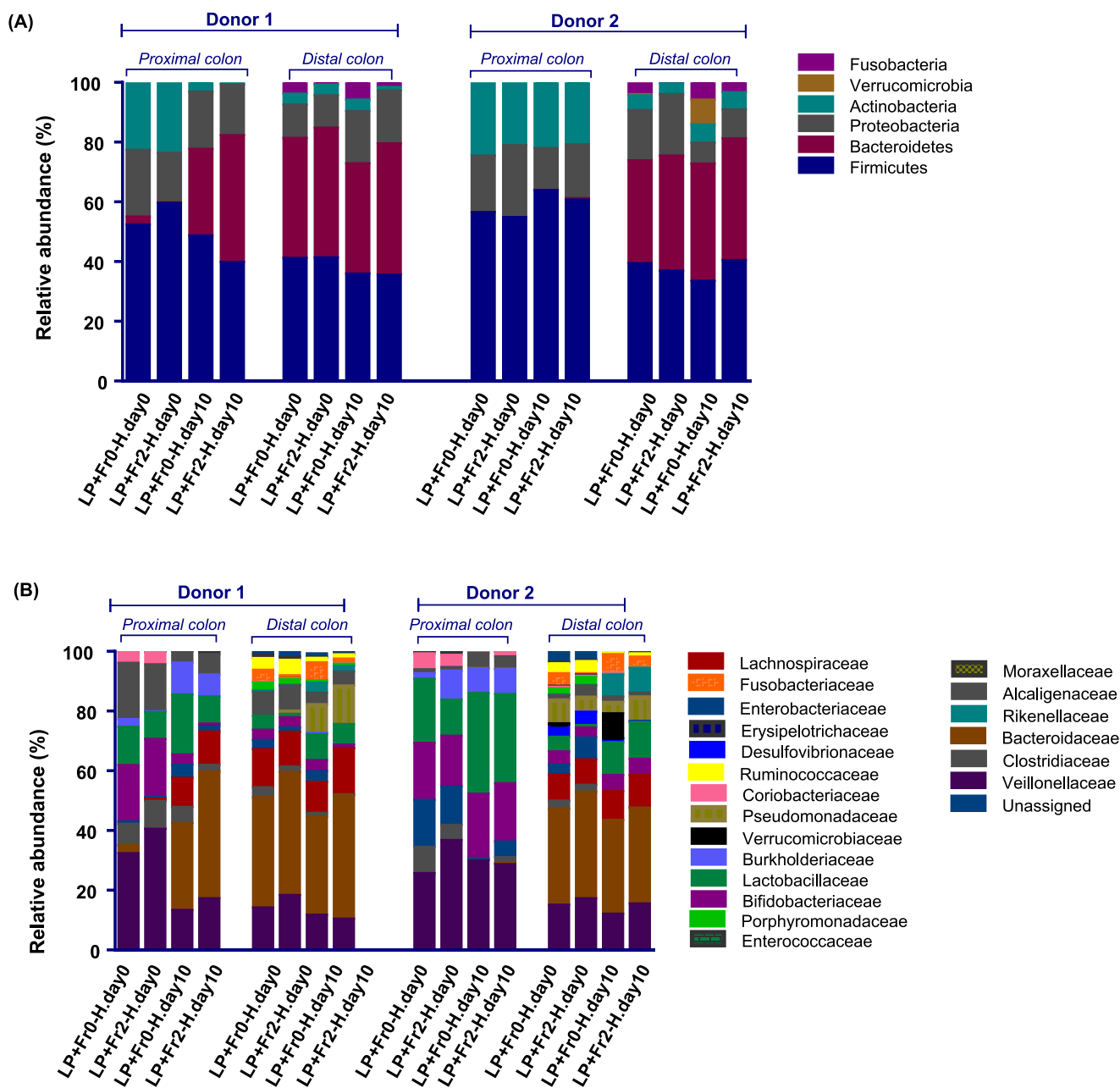


Fig. 4. Population profile from 16S rRNA gene sequenced after supplementing growth medium with insoluble hydrolysates (LP+Fr0-H and LP+Fr2-H) in a 10 day-fermentation with SHIME®. (A): Relative abundance at phylum level (B): Relative abundance at family level. LP+Fr0-H and LP+Fr2-H are the insoluble hydrolysates obtained from acid precipitation of digested LP+Fr0 and LP+Fr2, respectively.

affect the metabolites produced from their fermentation in the colon. Although extent of protein glycation does not alter the level of short-chain fatty acids and ammonia produced by the gut microbiota, it is unclear if the same would hold true for other protein fermentation products like hydrogen sulphide, phenols, or indoles. Therefore, further investigation is needed to ascertain whether these peptides may produce beneficial or detrimental effect in the colon or systemically.

Higher temperature and longer incubation time might produce more extensively crosslinked glycated proteins and Maillard reaction products that might be utilized differently by the gut microbiota. Evaluation of the effect of harsher glycation conditions on the gut microbiota is needed. Additionally, further studies of how these metabolites affect the host's metabolism are warranted. It is noteworthy that the gut microbiota was exposed to same amount of glycated lentil protein hydrolysates. Considering that glycation can reduce protein digestibility, it is

expected that the amount of ileal effluent reaching the colon will differ based on the extent of glycation. Further investigation must be carried out to evaluate the effect of the difference in effluent amount to fully understand the effect of ingesting the same amount of differently glycated proteins.

#### CRediT authorship contribution statement

**Ruth T. Boachie:** Conceptualization, Methodology, Investigation, Formal analysis, Writing – original draft, Writing – review & editing, Visualization. **Edoardo Capuano:** Conceptualization, Methodology, Visualization, Writing – review & editing. **Teresa Oliviero:** Conceptualization, Methodology, Supervision, Writing – review & editing. **Chibuikwe C. Udenigwe:** Conceptualization, Methodology, Supervision, Writing – review & editing. **Vincenzo Fogliano:** Conceptualization,

Methodology, Supervision, Writing – review & editing.

## Declaration of Competing Interest

The authors declare that they have no known competing financial interests or personal relationships that could have appeared to influence the work reported in this paper.

## Data availability

Data will be made available on request.

## Acknowledgement

The authors would like to acknowledge Hristiyanna Ivanova's help with simulated *in vitro* digestion. We would like to thank Erik Meulenbroeks, Christos Fryganas, and Geert Meijer for the outstanding technical support in using the SHIME® and the HPLC.

## Funding

This project was supported by Wageningen University & Research and Natural Sciences and Engineering Research Council of Canada (NSERC), Canada.

## Ethics statement

Authors declare that no human or animal subjects were included in this study.

## Appendix A. Supplementary material

Supplementary data to this article can be found online at <https://doi.org/10.1016/j.jff.2023.105667>.

## References

- Aguirre, M., Eck, A., Koenen, M. E., Savelkoul, P. H. M., Budding, A. E., & Venema, K. (2016). Diet drives quick changes in the metabolic activity and composition of human gut microbiota in a validated *in vitro* gut model. *Research in Microbiology*, 167(2), 114–125. <https://doi.org/10.1016/j.resmic.2015.09.006>
- Amaretti, A., Gozzoli, C., Simone, M., Raimondi, S., Righini, L., Pérez-Brocá, V., ... Rossi, M. (2019). Profiling of Protein Degraders in Cultures of Human Gut Microbiota. *Frontiers in Microbiology*, 10. <https://doi.org/10.3389/fmicb.2019.02614>.
- Ashaolu, T. J., Saibandith, B., Yupanqui, C. T., & Wichienchot, S. (2019). Human colonic microbiota modulation and branched chain fatty acids production affected by soy protein hydrolysate. *International Journal of Food Science and Technology*, 54(1), 141–148. <https://doi.org/10.1111/ijfs.13916>
- Barbana, C., & Boye, J. I. (2013). *In vitro* protein digestibility and physico-chemical properties of flours and protein concentrates from two varieties of lentil (*Lens culinaris*). *Food and Function*, 4(2), 310–321. <https://doi.org/10.1039/c2fo30204g>
- Boachie, R. T., Okagu, O. D., Abioye, R., Hüttmann, N., Oliviero, T., Capuano, E., Fogliano, V., & Udenigwe, C. (2022). Lentil protein and tannic acid interaction limits *in vitro* peptic hydrolysis and alters peptidomic profiles of the proteins. *Journal of Agricultural and Food Chemistry*, 70(21), 6519–6529. [https://doi.org/10.1021/ACS.JAFC.2C00197/SUPPL\\_FILE/JF2C00197\\_SI\\_001.PDF](https://doi.org/10.1021/ACS.JAFC.2C00197/SUPPL_FILE/JF2C00197_SI_001.PDF)
- Bolyen, E., Rideout, J. R., Dillon, M. R., Bokulich, N. A., Abnet, C. C., Al-Ghalith, G. A., ... Caporaso, J. G. (2019). Reproducible, interactive, scalable and extensible microbiome data science using QIIME 2. *Nature Biotechnology*, 37(8). <https://doi.org/10.1038/s41587-019-0209-9>
- Borrelli, R. C., & Fogliano, V. (2005). Bread crust melanoidins as potential prebiotic ingredients. *Molecular Nutrition and Food Research*, 49(7). <https://doi.org/10.1002/mnfr.200500011>
- Bui, T. P. N., Ritari, J., Boeren, S., de Waard, P., Plugge, C. M., & de Vos, W. M. (2015). Production of butyrate from lysine and the Amadori product fructoselysine by a human gut commensal. *Nature Communications*, 6. <https://doi.org/10.1038/NCOMMS10062>
- Cui, H., Yu, J., Zhai, Y., Feng, L., Chen, P., Hayat, K., ... Ho, C. T. (2021). Formation and fate of Amadori rearrangement products in Maillard reaction. *Trends in Food Science and Technology*, 115. doi: 10.1016/j.tifs.2021.06.055.
- L. Day J.A. Cakebread S.M. Loveday food proteins from animals and plants: Differences in the nutritional and functional properties *Trends in Food Science and Technology*, 119, 428–442. doi: 10.1016/j.tifs.2021.12.020.
- de Oliveira, F. C., dos Coimbra, J. S., de Oliveira, R., Zuñiga, E. B., G, A. D., & Rojas, E. E. G. (2016). Food protein-polysaccharide conjugates obtained via the Maillard reaction: a review. *Critical Reviews in Food Science and Nutrition*, 56(7), 1108–1125. <https://doi.org/10.1080/10408398.2012.755669>
- Delatour, T., Hegele, J., Parisod, V., Richoz, J., Maurer, S., Steven, M., & Buettler, T. (2009). Analysis of advanced glycation endproducts in dairy products by isotope dilution liquid chromatography-electrospray tandem mass spectrometry. The particular case of carboxymethyllysine. *Journal of Chromatography A*, 1216(12), 2371–2381. <https://doi.org/10.1016/j.chroma.2009.01.011>
- Di Stefano, E., Tsopmo, A., Oliviero, T., Fogliano, V., & Udenigwe, C. C. (2019). Bioprocessing of common pulses changed seed microstructures, and improved dipeptidyl peptidase-IV and  $\alpha$ -glucosidase inhibitory activities. *Scientific Reports*, 9(1), 1–13. <https://doi.org/10.1038/s41598-019-51547-5>
- Diether, N. E., & Willing, B. P. (2019). Microbial fermentation of dietary protein: An important factor in diet–microbe–host interaction. *Microorganisms*, 7(1). MDPI AG. doi: 10.3390/microorganisms7010019.
- Dominika, Š., Arjan, N., Karyn, R. P., & Henryk, K. (2011). The study on the impact of glycated pea proteins on human intestinal bacteria. *International Journal of Food Microbiology*, 145(1), 267–272. <https://doi.org/10.1016/j.ijfoodmicro.2011.01.002>
- Duncan, S. H., Iyer, A., & Russell, W. R. (2021). Impact of protein on the composition and metabolism of the human gut microbiota and health. *Proceedings of the Nutrition Society*, 80(2). <https://doi.org/10.1017/S0029665120008022>
- Fan, P., Li, L., Rezaei, A., Eslamfam, S., Che, D., & Ma, X. (2015). Metabolites of Dietary Protein and Peptides by Intestinal Microbes and their Impacts on Gut. *Current Protein & Peptide Science*, 16(7). <https://doi.org/10.2174/1389203716666150630133657>
- Feng, J., Berton-Carabin, C. C., Ataç Mogol, B., Schroën, K., & Fogliano, V. (2021). Glycation of soy proteins leads to a range of fractions with various supramolecular assemblies and surface activities. *Food Chemistry*, 343. <https://doi.org/10.1016/j.foodchem.2020.128556>
- Feng, J., Berton-Carabin, C. C., Fogliano, V., & Schroën, K. (2022). Maillard reaction products as functional components in oil-in-water emulsions: A review highlighting interfacial and antioxidant properties. *Trends in Food Science and Technology*, 121. doi: 10.1016/j.tifs.2022.02.008.
- Hellwig, M., Bunzel, D., Huch, M., Franz, C. M. A. P., Kulling, S. E., & Henle, T. (2015). Stability of individual Maillard reaction products in the presence of the human colonic microbiota. *Journal of Agricultural and Food Chemistry*, 63(30). <https://doi.org/10.1021/acs.jafc.5b01391>
- Inan-Eroglu, E., Ayaz, A., & Buyuktuncer, Z. (2020). Formation of advanced glycation endproducts in foods during cooking process and underlying mechanisms: A comprehensive review of experimental studies. *In Nutrition Research Reviews*, 33(1). <https://doi.org/10.1017/S0954422419000209>
- Koper, J. E. B., Loonen, L. M. P., Wells, J. M., Troise, A. D., Capuano, E., & Fogliano, V. (2019). Polyphenols and Tryptophan Metabolites Activate the Aryl Hydrocarbon Receptor in an *in vitro* Model of Colonic Fermentation. *Molecular Nutrition and Food Research*. <https://doi.org/10.1002/mnfr.201800722>
- Kutzli, L., Weiss, J., & Gibis, M. (2021). Glycation of plant proteins via Maillard reaction: Reaction chemistry, technofunctional properties, and potential food application. *Foods*, 10(2). <https://doi.org/10.3390/foods10020376>
- Li, Y., Zhong, F., Ji, W., Yokoyama, W., Shoemaker, C. F., Zhu, S., & Xia, W. (2013). Functional properties of Maillard reaction products of rice protein hydrolysates with mono-, oligo- and polysaccharides. *Food Hydrocolloids*, 30(1), 53–60. <https://doi.org/10.1016/j.foodhyd.2012.04.013>
- Martins, S. I. F. S., Jongen, W. M. F., & Van Boekel, M. A. J. S. (2000). A review of Maillard reaction in food and implications to kinetic modeling. *Trends in Food Science and Technology*, 11(9–10). doi: 10.1016/S0924-2244(01)00022-X.
- Minekus, M., Alminger, M., Alvito, P., Ballance, S., Bohn, T., Bourlieu, C., ... Brodtkorb, A. (2014). A standardised static *in vitro* digestion method suitable for food – an international consensus. *Food and Function*, 5(6), 1113–1124. <https://doi.org/10.1039/c3fo60702j>
- Mossé, J. (1990). Nitrogen to protein conversion factor for ten cereals and six legumes or oilseeds. A reappraisal of its definition and determination. Variation according to species and to seed protein content. *Journal of Agricultural and Food Chemistry*, 38(1), 18–24. <https://doi.org/10.1021/jf00091a004>
- Neis, E. P. J. G., Dejong, C. H. C., & Rensen, S. S. (2015). The role of microbial amino acid metabolism in host metabolism. *Nutrients*, 7(4), 2930–2946. MDPI AG. doi: 10.3390/nu7042930.
- Nielsen, P. M., Petersen, D., & Dambmann, C. (2001). Improved method for determining food protein degree of hydrolysis. *Journal of Food Science*, 66(5), 642–646. <https://doi.org/10.1111/j.1365-2621.2001.tb04614.x>
- Olagunju, A. I., Omoba, O. S., Enujiugha, V. N., Alashi, A. M., & Aluko, R. E. (2021). Thermoase-hydrolysed pigeon pea protein and its membrane fractions possess *in vitro* bioactive properties (antioxidative, antihypertensive, and antidiabetic). *Journal of Food Biochemistry*, 45(3). <https://doi.org/10.1111/JFBC.13429>
- Oliphant, K., & Allen-Vercoe, E. (2019). Macronutrient metabolism by the human gut microbiome: Major fermentation by-products and their impact on host health. *Microbiome*, 7(1). <https://doi.org/10.1186/s40168-019-0704-8>
- Peled, S., & Livney, Y. D. (2021). The role of dietary proteins and carbohydrates in gut microbiome composition and activity: A review. *Food Hydrocolloids*, 120. <https://doi.org/10.1016/j.foodhyd.2021.106911>
- Rovalino-Córdova, A. M., Fogliano, V., & Capuano, E. (2020). Effect of bean structure on microbiota utilization of plant nutrients: An *in-vitro* study using the simulator of the human intestinal microbial ecosystem (SHIME®). *Journal of Functional Foods*. <https://doi.org/10.1016/j.jff.2020.104087>
- Sari, Y. W., Mulder, W. J., Sanders, J. P. M., & Bruins, M. E. (2015). Towards plant protein refinery: Review on protein extraction using alkali and potential enzymatic assistance. *Biotechnology Journal*, 10(8). <https://doi.org/10.1002/biot.201400569>

- Shevkani, K., Singh, N., Chen, Y., Kaur, A., & Yu, L. (2019). Pulse proteins: Secondary structure, functionality and applications. *Journal of Food Science and Technology*, 56(6), 2787–2798. <https://doi.org/10.1007/s13197-019-03723-8>
- Taciak, M., Barszcz, M., Świąch, E., Tuśnio, A., & Bachanek, I. (2017). Interactive effects of protein and carbohydrates on production of microbial metabolites in the large intestine of growing pigs. *Archives of Animal Nutrition*, 71(3). <https://doi.org/10.1080/1745039X.2017.1291202>
- Troise, A. D., Fiore, A., Wiltafsky, M., & Fogliano, V. (2015). Quantification of Ne-(2-Furoylmethyl)-l-lysine (furosine), Ne-(Carboxymethyl)-l-lysine (CML), Ne-(Carboxyethyl)-l-lysine (CEL) and total lysine through stable isotope dilution assay and tandem mass spectrometry. *Food Chemistry*, 188, 357–364. <https://doi.org/10.1016/j.foodchem.2015.04.137>
- A. Tyakht v., Kostryukova, E. S., Popenko, A. S., Belenikin, M. S., Pavlenko, A. v., Larin, A. K., ... Govorun, V. M. (2013). Human gut microbiota community structures in urban and rural populations in Russia. *Nature Communications*, 4. doi: 10.1038/ncomms3469.
- Van Boekel, M. A. J. S. (2001). Kinetic aspects of the Maillard reaction: A critical review. *Nahrung - Food*, 45(3). [https://doi.org/10.1002/1521-3803\(20010601\)45:3<150::AID-FOOD150>3.0.CO;2-9](https://doi.org/10.1002/1521-3803(20010601)45:3<150::AID-FOOD150>3.0.CO;2-9)
- Van Den Abbeele, P., Taminiau, B., Pinheiro, I., Duysburgh, C., Jacobs, H., Pijls, L., & Marzorati, M. (2018). Arabinosylo-oligosaccharides and inulin impact inter-individual variation on microbial metabolism and composition, which immunomodulates human cells. *Journal of Agricultural and Food Chemistry*, 66(5), 1121–1130. <https://doi.org/10.1021/ACS.JAFC.7B04611>
- van der Lugt, T., Venema, K., van Leeuwen, S., Vrolijk, M. F., Opperhuizen, A., & Bast, A. (2020). Gastrointestinal digestion of dietary advanced glycation endproducts using an: In vitro model of the gastrointestinal tract (TIM-1). *Food and Function*, 11(7), 6297–6307. <https://doi.org/10.1039/d0fo00450b>
- Wang, C., Li, J., Li, X., Chang, C., Zhang, M., Gu, L., Su, Y., & Yang, Y. (2019). Emulsifying properties of glycation or glycation-heat modified egg white protein. *Food Research International*. <https://doi.org/10.1016/j.foodres.2019.01.047>
- Wrodnigg, T. M., & Eder, B. (2001). *The Amadori and Heyns rearrangements: Landmarks in the history of carbohydrate chemistry or unrecognized synthetic opportunities?* (pp. 115–152). doi: 10.1007/3-540-44422-X\_6.
- Wu, Y., Dong, L., Liu, H., Niu, Z., Zhang, Y., & Wang, S. (2020). Effect of glycation on the structural modification of  $\beta$ -conglycinin and the formation of advanced glycation end products during the thermal processing of food. *European Food Research and Technology*, 246(11). <https://doi.org/10.1007/s00217-020-03570-4>
- Xu, Y., Zhao, Y., Wei, Z., Zhang, H., Dong, M., Huang, M., Han, M., Xu, X., & Zhou, G. (2020). Modification of myofibrillar protein via glycation: Physicochemical characterization, rheological behavior and solubility property. *Food Hydrocolloids*, 105. <https://doi.org/10.1016/j.foodhyd.2020.105852>
- Yang, Q., Wang, Y., Yang, M., Liu, X., Lyu, S., Liu, B., Liu, J., & Zhang, T. (2022). Effect of glycation degree on the structure and digestion properties of ovalbumin: A study of amino acids and peptides release after in vitro gastrointestinal simulated digestion. *Food Chemistry*, 373(PB), Article 131331. <https://doi.org/10.1016/j.foodchem.2021.131331>
- Yang, Y., Wu, H., Dong, S., Jin, W., Han, K., Ren, Y., & Zeng, M. (2018). Glycation of fish protein impacts its fermentation metabolites and gut microbiota during in vitro human colonic fermentation. *Food Research International*, 113, 189–196. <https://doi.org/10.1016/j.foodres.2018.07.015>
- Zha, F., Dong, S., Rao, J., & Chen, B. (2019). The structural modification of pea protein concentrate with gum Arabic by controlled Maillard reaction enhances its functional properties and flavor attributes. *Food Hydrocolloids*, 92(October 2018), 30–40. doi: 10.1016/j.foodhyd.2019.01.046.
- Zha, F., Yang, Z., Rao, J., & Chen, B. (2019). Gum Arabic-mediated synthesis of glyco-pea protein hydrolysate via Maillard reaction improves solubility, flavor profile, and functionality of plant protein. *Journal of Agricultural and Food Chemistry*, 67(36), 10195–10206. <https://doi.org/10.1021/acs.jafc.9b04099>
- Zhang, G., Huang, G., Xiao, L., & Mitchell, A. E. (2011). Determination of advanced glycation endproducts by LC-MS/MS in raw and roasted almonds (*Prunus dulcis*). *Journal of Agricultural and Food Chemistry*, 59(22). <https://doi.org/10.1021/jf202515k>
- Zhang, G., Sun, C., Song ru, J., Jin, W., Tang, Yi, Zhou, Y., Yong, D., & Song, L. (2023). Glycation of whey protein isolate and stachyose modulates their in vitro digestibility: Promising prebiotics as functional ingredients. *Food Bioscience*, 52. <https://doi.org/10.1016/j.fbio.2023.102379>
- Zhao, D., Li, L., Le, T. T., Larsen, L. B., Su, G., Liang, Y., & Li, B. (2017). Digestibility of glyoxal-glycated  $\beta$ -casein and  $\beta$ -lactoglobulin and distribution of peptide-bound advanced glycation end products in gastrointestinal digests. *Journal of Agricultural and Food Chemistry*, 65(28), 5778–5788. [https://doi.org/10.1021/ACS.JAFC.7B01951/ASSET/IMAGES/LARGE/JF-2017-01951T\\_0008.JPEG](https://doi.org/10.1021/ACS.JAFC.7B01951/ASSET/IMAGES/LARGE/JF-2017-01951T_0008.JPEG)